

The Interaction between an Edge and an Embedded Parallel Crack in a Structural Component

Qin Ma^{1*}, Cesar Levy² and Mordechai Perl³

¹ Department of Mechanical Engineering, Walla Walla University, Walla Walla, Washington, USA

² Department of Mechanical and Materials Engineering, Florida International University, Miami, Florida, USA

³ Mechanical Engineering Department, Ben Gurion University of the Negev, Beer-Sheva, ISRAEL

Email: qin.ma@wallawalla.edu

Abstract. Parallel cracks are often detected in various structural components using non-destructive methods. In the case of non-aligned parallel cracks, on-site service needs to decide whether they should be treated as coalesced or separate multiple cracks for Fitness-for-Service. Criteria and standards for the adjustment of multiple nonaligned cracks are very different from one another in existing resources. Furthermore, those criteria and standards are often derived from on-site service experience without rigorous and systematic verification. Based on this observation, the interaction between an edge and an embedded parallel crack is investigated to correlate criteria and standards from various resources in order to recommend the usage of those standards for the purpose of Fitness-for-Service. In this study, depending on the crack ratio a_1/a_2 , what may be deemed conservative by one standard, leading to aligned cracks for a given separation distance, H/a_2 and S/a_2 , may be deemed non-conservative, or non-aligned, by another standard. Examples are given to show this phenomenon.

Keywords: parallel cracks; non-aligned; Fitness-for-Service; linear elastic fracture mechanics (LEFM)

Nomenclature

a_1 - half length of embedded internal crack

a_2 - length of edge crack

H - vertical crack separation distance

S - horizontal crack separation distance

E - Young's modulus

K_I - mode I SIF

K_{IB} - mode I SIF due at the edge crack tip B

K_0 - Normalizing SIF

p - applied tensile load

GREEK SYMBOLS

ν - Poisson's ratio

σ_y - yield stress

1 Introduction

Civil infrastructure systems such as older bridges in the United States, as in many other countries, are prone to structural damage due to repeated high load carrying capacities and due to the presence of an aggressive environment over long periods of time. According to a 2017 infrastructure report by the ASCE [1], close to 10% of the nation's bridges are rated structurally deficient. Biezma and Schanack [2] pointed out that structural damage in these bridges (e.g. cracks, corrosion, or excessive deformation) in critical structural members could compromise the structure and lead to disastrous failures. One well-studied case was the Point Pleasant Bridge in West Virginia that collapsed suddenly killing 46 people in December, 1967. Although this and other bridges that failed previously by brittle fracture were studied extensively, the bridge-building industry did not pay particular attention to the possibility of brittle fractures in bridges until the failure of the Point Pleasant Bridge as reported by Barsom and Rolfe [3]. The final National Transportation and Safety Board (NTSB) report indicated that the initial flaw was due to fatigue, stress-corrosion cracking, and/or corrosion fatigue [4].

Since the time of the Point Pleasant Bridge failure, other brittle fractures have occurred in steel bridges and other types of structures as a result of unsatisfactory fabrication methods, design details, or material properties (Engineering News Record [5-6]). Fisher [7] has described numerous fractures in a text on case studies and has shown that of various damage mechanisms in steel bridges, fatigue cracks are extremely common.

In the preceding situations as well as in many other structural components, the interaction of multiple cracks plays an important role in the degradation of such civil structures and plant components, especially in the case of stress corrosion cracking (SCC) and fatigue (see for example, Okamura et al. [8], Kamaya and Haruna [9]). The Fitness-for-Service standards require the characterization of multiple cracks in order to evaluate the structural integrity of the cracked components using fracture mechanics concepts. Multiple cracks must first be identified as to whether they are on the same cross-section plane to be considered aligned cracks or whether they are on parallel planes and considered to be non-aligned parallel cracks, using crack alignment rules. There are multiple crack alignment rules that can be considered for in-service evaluations, such as those found in the American Society of Mechanical Engineers Boiler and Pressure Vessel Code Section XI [10], Guide to methods for assessing the acceptability of cracks in metallic structures in British Standards [11], European Fitness-for-Service Network, FITNET [11], American Petroleum Institute (API) 579-1/ASME FFS-1 [13], Rules on Fitness-for-Service for Nuclear Power Plant Components in the Japan Society of Mechanical Engineers S NA1-2008 [14]. These rules differ from each other and some alignment rules may provide overly conservative results while others give non-conservative assessments.

In recent years there have been some intensive studies regarding the interaction of multiple non-aligned cracks in cases of two offset parallel embedded cracks contained in an infinitely large steel plate. For example, Kamaya [15] studied the growth evaluation of multiple interacting surface cracks by combination of numerical methods and experimental studies. Hasegawa et al. [16] studied the interaction of two parallel embedded non-aligned cracks for Fitness-for-Service based on LEFM. In their most recent studies Hasegawa et al. [17-18], Miyazaki et al. [19], and Suga et al. [20-21] considered plastic collapse behavior for dissimilar non-aligned cracks.

However, none of the aforementioned investigations addressed, in detail, the interaction of multiple cracks where one of the cracks was an edge crack. Based on this observation, the objective of this study is to investigate the influence of an embedded crack on the fracture behavior of an edge crack in an infinitely large half plate. Specifically, the stress intensity factors (SIFs) at the inner tip of the edge crack have been studied for a wide range of the NVSD $H/a_2 = 0.4$ to 2.0 and the NHSD of $S/a_2 = -0.5$ to 2.0 (see Fig. 1) between cracks on parallel planes based on the principle of linear elastic fracture mechanics (LEFM).

2 The Mathematical Model

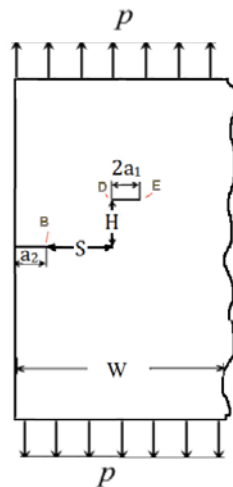


Figure 1. A flat plate with two non-aligned through-wall cracks, one edge crack and the other embedded crack. The far-field stress is p

Figure 1 depicts a flat plate, representing the cracked structural component, containing an edge crack and an embedded internal crack. The plate is assumed to be made of steel with Young's modulus $E=200$ GPa, Poisson's ratio $\nu=0.3$, and yield stress $\sigma_y = 304$ MPa. The remote uniaxial tensile stress load is taken as $p = 2$ KPa.

The plate is assumed elastic, infinitely long and very wide (W), so that the KI values are not affected by the plate's dimensions. The edge crack is of length a_2 , and the embedded internal crack is of length $2a_1$. The cracks are assumed to be perpendicular to the applied load. The cracks' HSD is S and their VSD is H . The points B, D and E represent the tip of the edge crack, the near tip of the embedded crack and the far tip of the embedded crack, respectively.

2.1 Finite Element Model and its Validation

The Finite Element (FE) model is solved using ANSYS FE standard code [22]. The majority of the plate is meshed, employing 2-D 6-noded triangular elements, while at the crack tip, singular elements are used. A global mesh of the entire plate, shown in Fig. 2(a), is generated using the 6-node triangular elements with plain strain conditions. The elements are varied in size, small near the crack regime and gradually increased when moving away from it as shown in Fig. 2(b). The 6-node triangular element has a quadratic displacement behavior and is well suited to model irregular meshes, specifically for a plate with an edge and an internally embedded crack.

Convergence tests were performed using the stress intensity factor as the convergence criterion. It is anticipated that the level of error will be, in most cases, less than 3% for meshes having more than 20,000 degrees of freedom (DOF). Typical meshes included about 10,000 elements with approximately 30,000 nodes and 60,000 DOFs. The option of automatic adjustment of elements shape and aspect ratio by the software was chosen. A typical stress contour, demonstrating the interaction behavior between the two cracks, is given in Fig. 3.

SIFs due to the remote tensile load are evaluated by the FE model using the KCALC command of ANSYS [22]. Stress intensity factors at the tip of the edge crack, K_{IB} , are obtained for various combinations of crack geometrical configurations and are normalized with respect to

$$K_0 = 1.12p\sqrt{\pi a_2} \quad (1)$$

where K_0 is the SIF solution for an edge crack in an infinitely large plate, Tada [23]. This normalizing factor would enable the comparison with various 2-D results under different loading conditions.

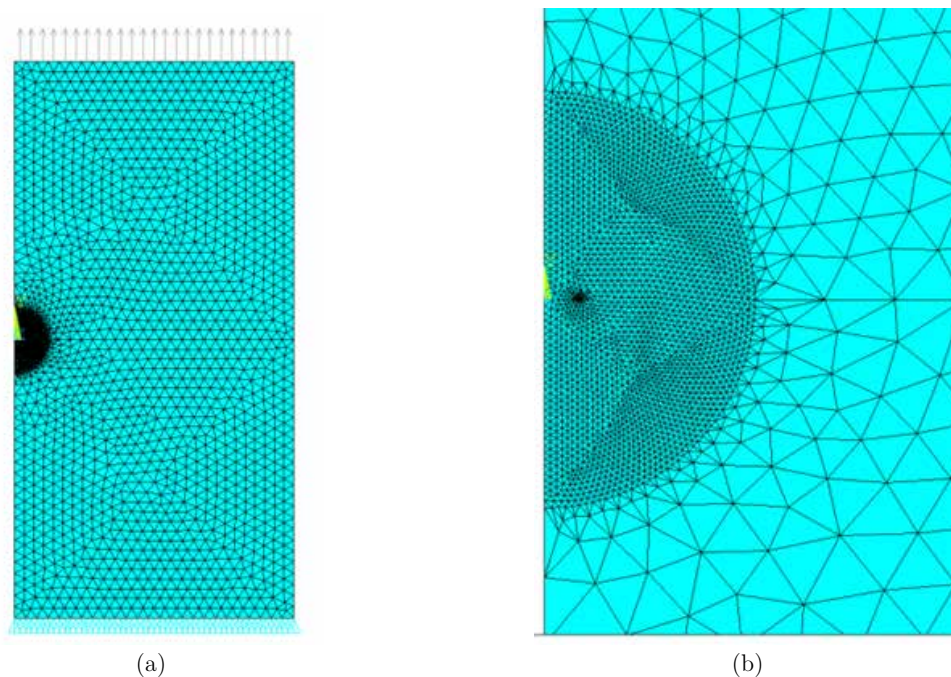


Figure 2. The Finite Element Model: (a) a typical global mesh; (b) a typical mesh at the vicinity of the cracks

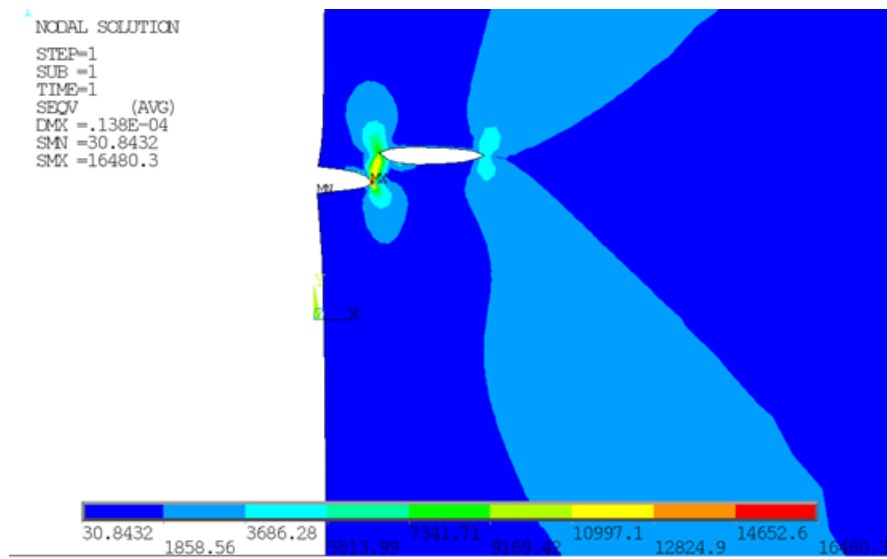


Figure 3. A typical contour plot of von Mises stress at the vicinity of the cracks

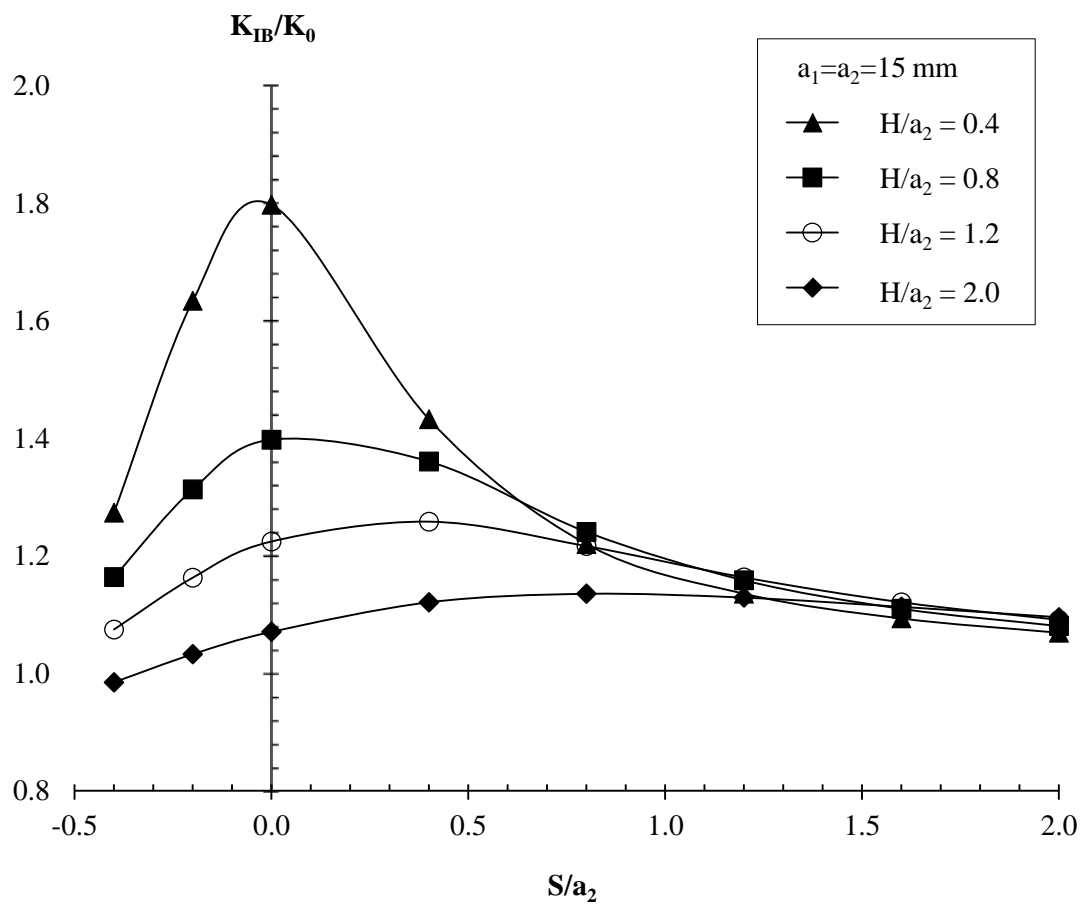


Figure 4. Normalized SIFs vs. S/a_2 as a function of H/a_2 for an edge crack ($a_2 = 15\text{mm}$; $2a_1=30\text{mm}$)

3 Results and Discussion

3.1 The Effect of Crack Spacing for Cracks of Similar Size

The SIFs at the inner tip of the edge crack, K_{IB} , as a function of the HSD, S , and the VSD, H , are presented in Fig. 4. The length of the edge crack is taken as $a_2 = 15$ mm and the embedded crack length is $2a_1 = 30$ mm; thus, in this case $a_1/a_2 = 1$. This case is somewhat analogous to the similar through-wall cracks (Hasegawa et al. [16]).

As long as the two cracks overlap, $S/a_2 \leq 0$, the normalized SIFs, K_{IB}/K_0 , increases as the embedded crack moves away from the edge crack, i.e., as NHSD increases, until reaching its maximum value. The NHSD at which K_{IB}/K_0 maxima occurs depends on the value of the NVSD. The smaller the NVSD is, the smaller the NHSD at which the maximum occurs. For example for $H/a_2=0.4$, $(K_{IB}/K_0)_{max}$ occurs near $S/a_2 \approx 0$, while for $H/a_2 = 2.0$, it occurs at about $S/a_2 \approx 1$. It can also be observed from Fig. 4 that the smaller the NVSD is, the sharper is the "rise" and "fall" of the K_{IB}/K_0 curve. It is evidently clear that the interaction of the two cracks is confined to a limited range of the HSD $S/a_2 = -0.4$ to 1.0 . As the HSD increases beyond $S/a_2 > 1$ the edge crack no longer "feels" the presence of the embedded crack, thus, each of the cracks can be treated separately for Fitness-for-Service considerations. Interestingly, the interaction for the present case produces a larger interaction region in comparison with the case of two embedded parallel cracks shown in Fig. 5 by Hasegawa et al. [16], which indicates that the edge-embedded crack interaction can be more critical for consideration in practical applications.

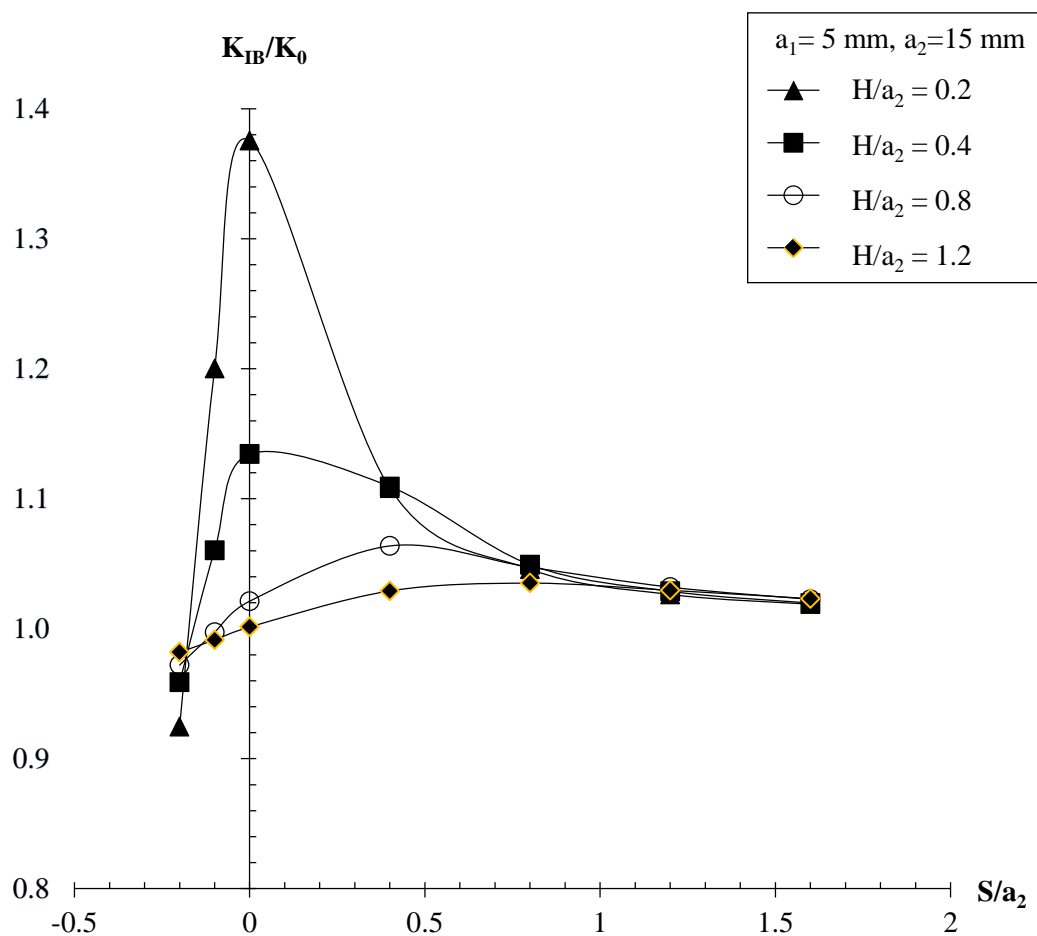


Figure 5. Normalized SIFs vs. S/a_2 as a function of H/a_2 for edge-embedded cracks ($a_2 = 15$ mm; $2a_1=10$ mm)

The interaction between an edge crack and an embedded crack is analysed for different crack size combinations as is demonstrated in the following cases. Figure 5 represents the interaction of an edge crack ($a_2 = 15$ mm) with a much smaller embedded crack of length $2a_1 = 10$ mm, thus the relative crack size is $a_1/a_2 = 1/3$. Considering the same range of NVSDs of $H/a_2 = 0.4$ to 1.2, it can be observed that the magnitude of the peak value of the normalized SIFs, K_{IB}/K_0 , has dropped from ~ 1.3 to ~ 1.1 for the case of $H/a_2 = 0.4$. The interaction range is much smaller, $S/a_2 = -0.1$ to 0.5, as compared to the previous case. Meaning, that if the vertical separation distance is kept constant and the relative size of the embedded crack a_1/a_2 is decreased, the amplification effect on the SIFs at the tip of the edge crack "dies out" much faster.

This fact is further illustrated in Fig. 6. In this case, the relative crack size is taken to be $a_1/a_2 = 0.5$, somewhat larger than the case shown in Fig. 5 but still smaller than the case shown in Fig. 4. The interaction range and the peak values fall, in this case, between the corresponding values in Figs. 4 and 5.

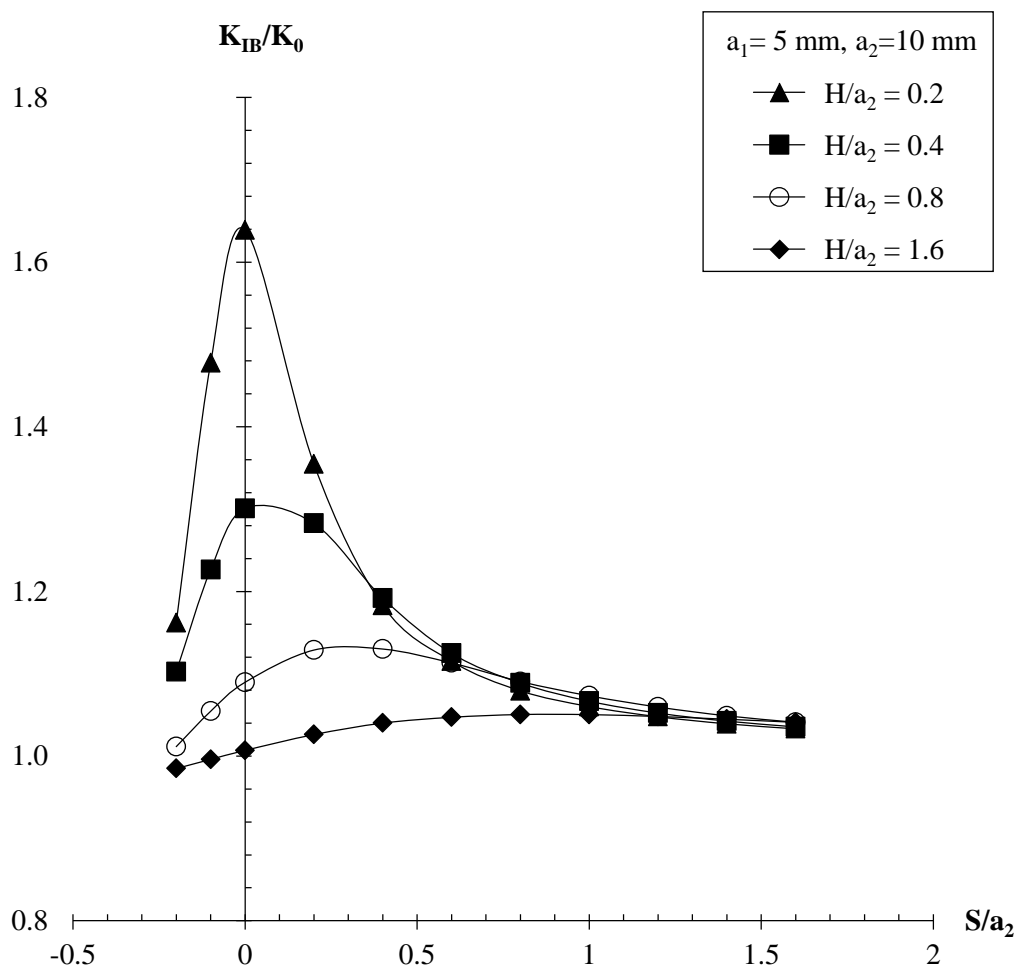


Figure 6. Normalized SIFs vs. S/a_2 as a function of H/a_2 for edge-embedded cracks ($a_2 = 10$ mm; $2a_1=10$ mm)

3.2 The Effects of Crack Spacing on Short Embedded Cracks

Figure 7 shows the effect of a very short embedded crack on the distribution of the SIFs at the tip of the edge crack where $a_2 = 15$ mm and $2a_1 = 5$ mm, and thus $a_1/a_2 = 1/6$. In this case, the overall effect on the edge crack is much weaker in comparison with the previous cases. This emphasizes that the influence of the embedded crack on the SIF of the edge crack is controlled by the relative crack size a_1/a_2 .

a_2 rather than be the absolute values of each crack size a_1 and a_2 . The amplification of the SIF at point B decrease rapidly as the relative crack size decreases. At the same time, when the two cracks become very close both vertically, e.g., $H/a_2 = 0.066$, as well as horizontally e.g., $S/a_2 = 0$, the two cracks may be considered as one.

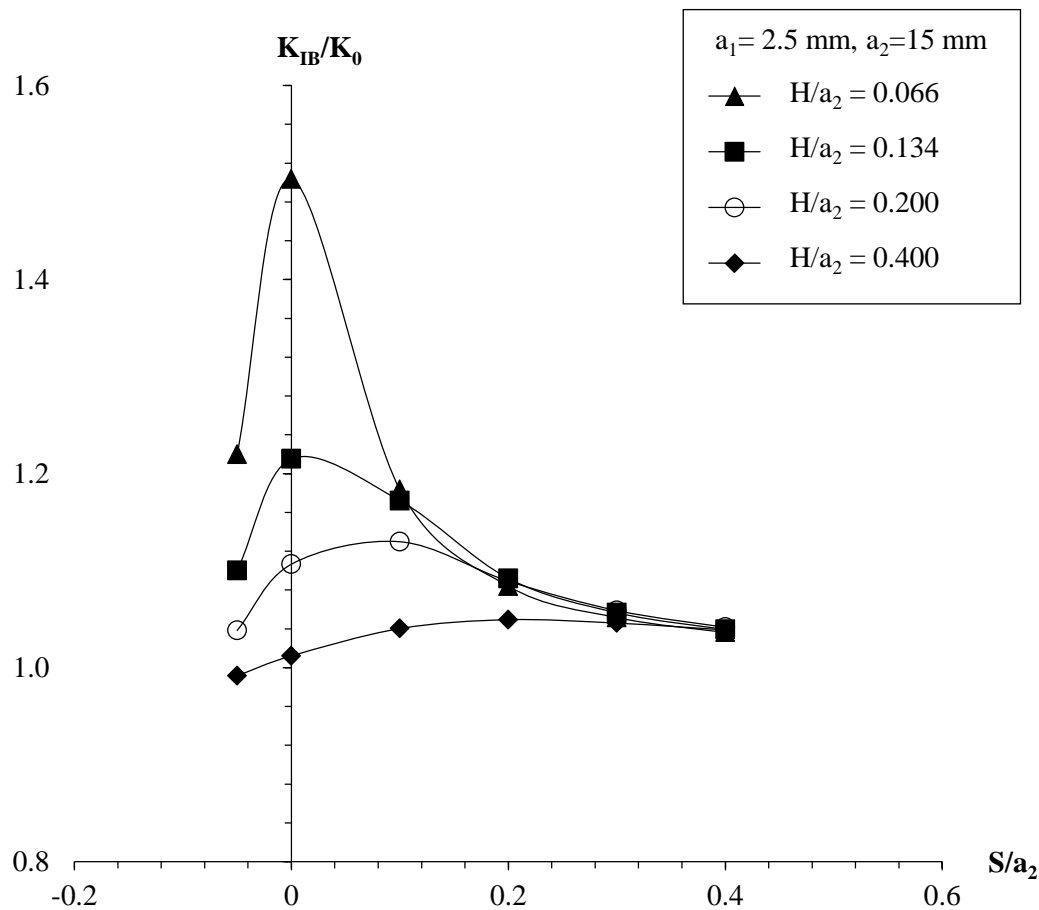


Figure 7. Normalized SIFs vs. S/a_2 as a function of H/a_2 for edge-embedded cracks ($a_2 = 15\text{mm}$; $2a_1=5\text{mm}$)

All the examples presented in Sections 3.1 and 3.2 prove that the interaction between the edge and the embedded cracks, which changes significantly from case to case, depends on multiple parameters: the cracks geometries and the horizontal and vertical separation distances. Therefore, it should be expected from any alignment rule to reflect this aspect by capturing these multifaceted parametric effects.

3.3 The Influence of Crack Alignment Rules

The Crack Alignment Rules are suggested methodologies by which parallel cracks are to be considered as either two separate cracks or as one long crack. Two such rules are considered in this work: The BritS criterion [11], and the FITNET (FFS) criterion [12].

The BritS criterion is given as

$$S_1 = \sqrt{S^2 + H^2} \leq a_1 + a_2 \tag{2}$$

where S_1 , segment BD in Fig. 1, is the distance connecting the crack tip of the edge crack and the tip of the embedded crack on the edge crack side. If S_1 is less than a_1+a_2 , then the two cracks are considered as one crack having a length of $(S+2a_1+a_2)$ in the Fitness-for-Service calculations. In the case where S_1 is greater than a_1+a_2 , then the cracks are considered as two separate cracks, and each is used to

determine which is the most dangerous in the Fitness-for-Service calculation. Since S_1 is the straight line distance between the closest two points of the edge crack and the embedded crack, this criterion considers the effect of separation parameters of both relative vertical distance, H/a_2 , and the relative horizontal distance, S/a_2 , as well as the relative crack size, a_1/a_2 , in an implicit manner.

The FITNET (FFS) criterion, on the other hand, is given as

$$H \leq \min(2a_1, a_2) \quad (3)$$

When H is the smaller of $2a_1$ and a_2 , then the cracks are considered as one long crack having a length $(S+2a_1+a_2)$ in the Fitness-for-Service calculation. When H is greater than the smaller of $2a_1$ and a_2 , then the cracks are considered as two separate cracks and each is used to determine which is the most dangerous in the Fitness-for-Service calculation. The FITNET (FFS) criterion accounts for the vertical separation distance only.

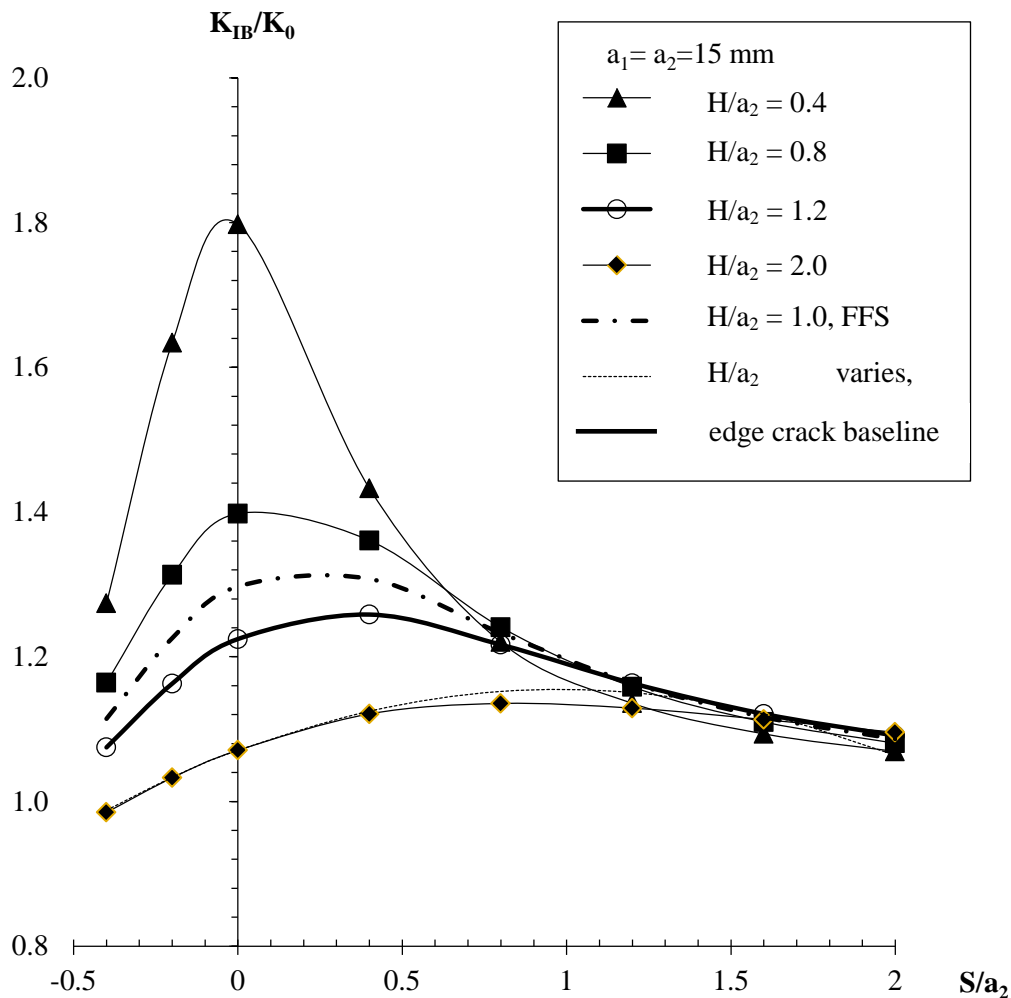


Figure 8. Normalized SIFs vs. S/a_2 as a function of H/a_2 for edge & embedded cracks ($a_2 = 15\text{mm}$; $2a_1=30\text{mm}$) with FITNET (FFS) standard and BritS standard

In order to compare the two criteria, it is necessary to convert the BritS criterion to one that involves H . Now, since

$$S_1 = \sqrt{S^2 + H^2} \quad (4)$$

solving for H from (3), using the inequality of Equation (2) and normalizing it to a_2 leads to:

$$\frac{H}{a_2} \leq \sqrt{\left(\frac{a_1}{a_2} + 1\right)^2 - \left(\frac{S}{a_2}\right)^2} \quad (5)$$

Therefore, based on the BritS criterion, each S/a_2 value corresponds to a different value of vertical separation distance H/a_2 .

Figure 8 shows the same results as presented in Fig. 4, but with the criteria included from two different Fitness-in-Service sources, the British Standards (BritS) [11] and the FITNET (FFS) [12], as well as the baseline normalized stress intensity factor value for the corner crack if the crack were by itself in the body. The baseline curve, in fact, represents the value of $(K_{IB}/K_0)_{\max}$ when the cracks are considered separate. The BritS criterion is presented as a thin small dashed curve on the graph; the FITNET (FFS) is represented on the graph as a dashed-dotted curve; and the baseline value is represented by the thick dashed curve.

The FITNET (FFS) does not include any effect from the horizontal separation dimension, S/a_2 , which is an important parameter that influences the SIF values. In fact, for the case presented in Fig. 8, the min $(2a_1, a_2)$ is $a_2=15\text{mm}$, and thus $H/a_2 = 1$. Thus, the thick dotted-dashed curve was obtained under a constant relative separation distance H/a_2 in the same manner as that for other cases under constant H/a_2 values. The BritS curve, which depends on the S/a_2 parameter, generates different H/a_2 results as S/a_2 varies. From left to right, the BritS curve is merged with the $H/a_2 = 2.0$ curve until $S/a_2 = 0.4$ before it separates from $H/a_2 = 2.0$ curve.

The two criteria apparently provide very different circumstances for the judgment of alignment vs. non-alignment for two parallel offset cracks. For certain crack separation conditions, one criterion may consider the same two cracks on parallel planes to act as one while the other criteria will suggest that the cracks be considered as separate ones (e.g., cracks having an $H/a_2 = 1.2$ and $S/a_2 = -0.2$ for $a_1/a_2 = 1$ in Fig. 8). The critical values from the BritS and the FITNET (FFS) rules as demonstrated in Fig. 8 clearly show that the FITNET (FFS) will provide a much higher barrier for the cracks to be judged as aligned ones. Thus, the FITNET (FFS) is a much more conservative rule. At the same time, the BritS provides much lower critical values of the SIFs. It thus provides relationally non-conservative results in Fitness-for-Service applications.

The results from other standards such as ASME B&PV Code Section XI [10], API 579-1 [13] and JSME S NA1-2008 [14], though not presented here, bear the same characteristic problems as have been discussed here.

When the other H/a_2 curves in Fig. 8 are compared to the baseline curve, it is noted that as H/a_2 becomes larger, meaning that the edge crack and the embedded crack are farther separated, the curves tend to the baseline curve. Until then, the cracks would be considered aligned. So, it stands to reason that one might consider defining the crack separation condition when the curves approach the baseline curve. If we were to consider, for instance, a 10% increase above the baseline curve as the standard for defining separated cracks while $dK_{\max}/dS < 0$, then this value would be reached when S/a_2 equals 2 for this particular instance where $a_1/a_2=1$. When we look at Fig. 8, it is noted that all the graphs appear to coalesce at $S/a_2 = 2$ and that is where both the BritS and the FITNET (FFS) rules appear to meet. Of course, the actual value of S/a_2 where the 10% criterion is met will depend on the ratio of a_1/a_2 (see, e.g., Fig. 7 where the 10% criterion is met at $S/a_2 = 0.2$ for $a_1/a_2 = 1/6$). One can also realize that by lowering the percentage criterion, one will delay when the cracks are considered separated. For example, in Fig. 6 where $a_1/a_2 = 0.5$, the 10% criterion is met at $S/a_2 = 0.7$; but if the criterion is reduced to 5%, then the separated crack criterion would be met at $S/a_2 = 1.3$.

4 Conclusions

In this study, a review of the stress intensity factor at the tip of an edge crack affected by an embedded crack on a parallel plane is evaluated. The amplification of the SIF at the tip of the edge crack is calculated as a function of the vertical and horizontal separation distance between the cracks as well as the cracks' relative size.

It is found that all three parameters affect the magnitude of the KIB at the tip of the edge crack as well as how far the embedded crack exhibits its "reach" on the edge crack. These two effects show that existing alignment rules used to evaluate the "Fitness-for-Service" do not agree and can lead to distinctly opposite results, which can prove to be disastrous. "As existing structures reach their design

life, there is considerable pressure to extend the life of these structures. Fracture mechanics can be used to establish the Fitness-for-Service or life extension of these structures on a rational technical basis” as pointed by Barsom and Rolfe [3]. Because fracture mechanics critically depends on the definition of the proper crack length to determine the SIF and, moreover, the correct SIF is necessary for the calculation of fatigue life, it is imperative that the Fitness-for-Service rules be accurate in defining the operative crack length. To this end, a Fitness-for-Service rule of 10% above the baseline curve for the fixed edge crack is proposed and some examples are given; but, depending on the percentage value taken, there can be great variance in the horizontal distance considered as the start of the separated crack region. Therefore, more work needs to be undertaken to bring any of these codes or the authors’ proposed separated crack rubric under one acceptable set of rules. As part of determining these unifying rules, the authors’ future work plans include issues such as how the embedded crack is affected by the edge crack and which rule may be used in a more practical manner. Both topics are under investigation in other studies by the authors.

Acknowledgments. The authors would like to thank the National Center for Supercomputing Applications (NCSA) at the University of Illinois at Urbana Champaign (UIUC) for computational and software support and resources. This research was supported in part by the National Science Foundation through its TeraGrid resources at NCSA. The first author (QM) would also like to express his deep gratitude to Walla Walla University for its support through its Faculty Development Grant. The authors acknowledge that this work is a modified and enhanced version of a paper presented at the PVP 2013 Conference in Paris, France [24].

References

1. American Society of Civil Engineers (ASCE) (2017), 2017 Infrastructure Report Card – Bridges, available: <https://www.infrastructurereportcard.org/wp-content/uploads/2017/01/BridgesFinal.pdf>
2. M.V. Biezma, and F. Schanack, “Collapse of steel bridges”, *Journal of Performance of Constructed Facilities*, vol. 21, no. 5, 2006, pp. 398-405.
3. J.M. Barsom, and S.T. Rolfe, *Fracture and Fatigue Control in Structures: Applications of Fracture Mechanics*, Third Edition, AMERICAN SOCIETY FOR TESTING AND MATERIALS, ASTM manual series: MNL 41, 1999, pp. 6-8.
4. NTSB (1968). Collapse of U.S. 35 Highway Bridge, Point Pleasant, West Virginia, Report No. NTSB- HAR-71-1, Oct. 4, 1968.
5. Engineering News Record. "State Cites Defective Steel in Bryte Bend Failure," vol. 185, no. 8, Aug. 20, 1970.
6. Engineering News Record. "Joint Redesign on Cracked Box Girder Cuts into Record Tied Arch's Beauty," vol. 188, no. 13, March 30, 1972.
7. J.W. Fisher, *Fatigue and Fracture in Steel Bridges--Case Studies*. John Wylie, 1984.
8. Y. Okamura, A. Sakashita, T. Fukuda, H. Yamashita, and T. Futami, “Latest SCC Issues of Core Shroud and recirculation Piping in Japanese BWRs”, *Trans. Of 17th Int. Conf. on Structural Mechanics in Reactor Technology (SMiRT 17)*, Prague, Paper WG01-1, 2003.
9. M. Kamaya, and T. Haruna, “Crack Initiation Model for Type 304 Stainless Steel in High Temperature Water,” *Corrosion Science*, vol. 48, pp. 2442-56, 2006.
10. ASME, *Boiler and Pressure Vessel Code Section XI, 2007 Edition*, American Society of Mechanical Engineers, 2007.
11. British Standards Institution, *Guide to Methods for Assessing the Acceptability of Flaws in Metallic Structures, BS 7910:2005*, British Standards Institution, 2005.
12. N. Taylor, M. Kocak, S. Webster, J.J. Janosch, R.A. Ainsworth, and R. Koers, *FITNET, European Fitness-for-Service Network GTC1- 2001-43049*, FITNET Consortium, 2001.
13. American Petroleum Institute, *Fitness-for-Service, API 579-1/ASME FFS-1*, American Society of Mechanical Engineers, 2007.
14. JSME, *Rules on Fitness-for-Service for Nuclear Power Plant, JSME S NA1-2008* (in Japanese), The Japan Society of Mechanical Engineers, 2008.
15. M. Kamaya, “Growth evaluation of multiple interacting surface cracks. Part I: Experiments and simulation of coalesced crack”, *Engineering Fracture Mechanics*, vol. 75, pp. 1350–1366, 2008.

16. K. Hasegawa, K. Saito, and K. Miyazaki, "Alignment Rule for Non-Aligned Flaws for Fitness-for Service Evaluations Based on LEFM", *ASME Journal of Pressure Vessel Technology*, vol. 131, article 041403-1, 2009.
17. K. Hasegawa, K. Saito, and K. Miyazaki, "Behavior of plastic collapse moments for pipes with two non-aligned flaws," in *Pressure Vessels and Piping Conference*, vol. 49200, pp. 355-361. 2010.
18. K. Hasegawa, K. Saito, and K. Miyazaki, "Plastic collapse loads for flat plates with dissimilar Non-aligned through-wall cracks," In *Pressure Vessels and Piping Conference*, vol. 44519, pp. 475-479. 2011.
19. K. Miyazaki, K. Hasegawa, and K. Saito, "Effect of flaw dimensions on ductile fracture behavior of non-aligned multiple flaws in a plate," In *Pressure Vessels and Piping Conference*, vol. 44519, pp. 459-465. 2011.
20. K. Suga, K. Miyazaki, S. Kawasaki, and Y. Arai, "Study on the interaction of multiple flaws in ductile fracture process," In *Pressure Vessels and Piping Conference*, vol. 44519, pp. 447-452. 2011.
21. K. Suga, K. Miyazaki, R. Senda, and M. Kikuchi, "Ductile fracture simulation of multiple surface flaws," In *Pressure Vessels and Piping Conference*, vol. 44519, pp. 433-439. 2011.
22. ANSYS, *Mechanical ANSYS Parametric Design Language*, 2012.
23. H. Tada, P.C. Paris, and G.R. and Irwin, *The Stress Analysis of Cracks Handbook, 3rd ed.*, American Society of Mechanical Engineers, 2000.
24. Q. Ma, C. Levy, and M. Perl, "An LEFM Based Study on the Interaction Between an Edge and an Embedded Parallel Crack", In *Pressure Vessels and Piping Conference*, vol. 55676, p. V003T03A046. American Society of Mechanical Engineers, 2013.